Indistinguishability of orbital angular-momentum modes in spontaneous parametric down-conversion

Geraldo Alexandre Barbosa*

Department of Electrical Engineering and Computer Science, Center for Photonic Communication and Computing, Northwestern University, 2145 North Sheridan Road, Evanston, Illinois 60208-3118, USA

(Received 3 December 2008; revised manuscript received 26 January 2009; published 8 May 2009)

Identification of light modes usually requires careful considerations of the collecting geometry. This is particularly true for states carrying orbital angular-momentum modes from spontaneous parametric down-conversion due to the entanglement of the signal and idler fields. A detailed understanding of the generated modes in a general case allows the design of efficient detection setups. This is true for distinct cases, e.g., when multiple samplings are performed by repeated state generation or in single-photon cryptography or quantum computation, where a photon state is generated within a short-time window and a single measurement is performed. Aspects of nonorthogonality of signal and idler modes and effects of restrictions on the collecting geometry are discussed in this work.

DOI: 10.1103/PhysRevA.79.055805 PACS number(s): 42.50.Tx, 42.50.Dv, 42.50.Ex

States of light carrying orbital angular momentum (OAM) are defined within spatial regions and their measurements require a careful probing of these regions to allow state identification. Sometimes, space limitations are not detrimental for state identification; in others, they are crucial. Light spin or circularly polarized light states, for example, needs a single wave-vector $\mathbf{k}$ approximation because "spin" is associated with a specific wave vector. Distinctly, OAM states demand finite regions of space for identification: a bundle of wave vectors is needed to specify a given mode. While this is an undisputed statement, sometimes specification of this geometry it is not a clear task and even the way one defines the photon concept plays a role. Figure 1 depicts wave vectors associated to an orbital angular-momentum mode near to a focal plane. Association of wave vectors with an orbital angular-momentum spatial mode $U_l(\mathbf{r},t)$ can be seen from the quantized electric field $\hat{\mathbf{E}}^{(+)}(\mathbf{r},t)$ decomposed in the plane-wave basis,

$$\hat{\mathbf{E}}^{(+)}(\mathbf{r},t)=\sum_{\mathbf{k}} l_E(\mathbf{k})\mathbf{e}_{\mathbf{k}}\hat{a}_{\mathbf{k}}e^{i(\mathbf{k}\cdot\mathbf{r}-\omega_{\mathbf{k}}t)}, \tag{1}$$

where $\mathbf{e}_{\mathbf{k}}$ is the unitary polarization vector and $l_E(\mathbf{k})=-i\sqrt{\hbar\omega_{\mathbf{k}}/(2\epsilon V)}$. Decompose $U_l(\mathbf{r},t)$ in the set of unitary matrices $U_{\mathbf{k},l}$ transforming between the two representations,

$$U_l(\mathbf{r},t)=\sum_{\mathbf{k}} U_{\mathbf{k},l}e^{i(\mathbf{k}\cdot\mathbf{r}-\omega_{\mathbf{k}}t)}, \tag{2}$$

they obey $\Sigma_l U_{\mathbf{k},l}U^*_{l,\mathbf{k}'}=\delta_{\mathbf{k},\mathbf{k}'}$. Writing $l_E(\mathbf{k})\mathbf{e}_{\mathbf{k}}\hat{a}_{\mathbf{k}}=\Sigma_{\mathbf{k}'}\delta_{\mathbf{k},\mathbf{k}'}l_E(\mathbf{k}')\mathbf{e}_{\mathbf{k}'}\hat{a}_{\mathbf{k}'}$ and replacing it in $\hat{\mathbf{E}}^{(+)}(\mathbf{r},t)$, one obtains

$$\hat{\mathbf{E}}^{(+)}(\mathbf{r},t)=\sum_l\left[\sum_{\mathbf{k}'}U^*_{l,\mathbf{k}'}l_E(\mathbf{k}')\mathbf{e}_{\mathbf{k}'}\hat{a}_{\mathbf{k}'}\right]\left[\sum_{\mathbf{k}}U_{\mathbf{k},l}e^{i(\mathbf{k}\cdot\mathbf{r}-\omega_{\mathbf{k}}t)}\right]$$
$$\equiv\sum_l\hat{\mathbf{c}}_l U_l(\mathbf{r},t). \tag{3}$$

In order to guarantee that an annihilated photon belongs to the spatial mode $U_l(\mathbf{r},t)$, the collection setup has to accept the set of wave vectors defining $\hat{\mathbf{c}}_l=\Sigma_{\mathbf{k}'}U^*_{l,\mathbf{k}'}l_E(\mathbf{k}')\mathbf{e}_{\mathbf{k}'}\hat{a}_{\mathbf{k}'}$ [or in $U_l(\mathbf{r},t)=\Sigma_{\mathbf{k}}U_{\mathbf{k},l}e^{i(\mathbf{k}\cdot\mathbf{r}-\omega_{\mathbf{k}}t)}$]. In cases where the experimental setup constrains the collected photon to a smaller set of wave vectors, what would be the effect on the distinguishability of different OAM modes in spontaneous parametric down-conversion (SPDC)? Understanding the generated modes in SPDC is necessary to better understanding this problem as well as the SPDC phenomenon itself. A brief presentation of SPDC will be done to introduce the necessary definitions and equations.

The phenomenon of SPDC has been well studied for some decades; it is described by the wave state [1]

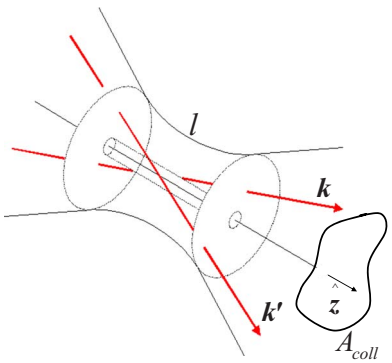

FIG. 1. (Color online) Wave vectors $\mathbf{k}$ and $\mathbf{k}'$ around the focus in a mode with angular momentum $l(\neq 0)$; they do not cross the z axis. Collecting a subset of the wave vectors defining the mode may lead to a poor distinguishability between modes with different l (e.g., detecting within area A_{coll}).

*g-barbosa@northwestern.edu

$$|\psi(t)\rangle = |0\rangle + \sum_{\sigma,\sigma'} \int d^3k' \int d^3k A_{\mathbf{k},\sigma;\mathbf{k}',\sigma'} l_E^{(*)}(\omega_{\mathbf{k}}) \times l_E^{(*)}(\omega'_{\mathbf{k}}) T(\Delta\omega) \tilde{\psi}_{lp}(\Delta\mathbf{k}) \hat{a}^\dagger(\mathbf{k},\sigma)\hat{a}^\dagger(\mathbf{k}',\sigma')|0\rangle, \quad (4)$$

where two down-converted photons are generated in an entangled state. $A_{\mathbf{k},\sigma;\mathbf{k}',\sigma'} = \chi^{(2)}_{1jk}[(\mathbf{e}_{\mathbf{k},\sigma})^*_j(\mathbf{e}_{\mathbf{k}',\sigma'})^*_k + (\mathbf{e}_{\mathbf{k}',\sigma'})^*_j(\mathbf{e}_{\mathbf{k},\sigma})^*_k]$ is the amplitude of the nonlinear polarizability that depends on the unitary polarization vectors (σ polarized) as well as on the nonlinear susceptibility. $T(\Delta\omega) = \exp[i\Delta\omega(t-t_{int}/2)]\sin(\Delta\omega t_{int}/2)/(\Delta\omega/2)$ is the time window function defining the $\Delta\omega$ range given the interaction time t_{int}, $\Delta\omega = \omega_{\mathbf{k}} + \omega'_{\mathbf{k}} - \omega_P$, $\Delta\mathbf{k} = \mathbf{k} + \mathbf{k}' - \mathbf{k}_P$. For $t_{int} \to \infty$, $T(\Delta\omega) \to \pi\delta(\Delta\omega)$. $\tilde{\psi}_{lp}(\Delta\mathbf{k}) = \int_V d^3r \psi_{lp}(\mathbf{r}) \exp(-i\Delta\mathbf{k}\cdot\mathbf{r})$ and ψ_{lp} is the field amplitude in $\mathbf{E}(\rho,\phi,z;t) = \psi_{lp}(\mathbf{r}) e^{i(k_P z - \omega_P t)}\hat{\mathbf{e}}$. For a pump beam with orbital angular momentum l [2], one has

$$\psi_{lp}(\rho,\phi,z) = \frac{A_{lp}}{\sqrt{1+(z/z_R)^2}} \left[\frac{\rho\sqrt{2}}{w(z)}\right]^l L_l^p\left[\frac{2\rho^2}{w(z)^2}\right] \times \exp\left[-\frac{\rho^2}{w(z)^2}\right] \times \exp\left\{-i\left[\frac{k\rho^2 z}{2(z^2+z_R^2)} + l\arctan(y/x)\right]\right\} \times \exp[i(2p+l+1)\arctan(z/z_R)]. \quad (5)$$

L_l^p is the associated Laguerre polynomial and $\rho^2 = x^2 + y^2$. $w(z)$ is the beam waist in a generic position z; z_R is the Rayleigh range. The spectral function $\tilde{\psi}_{lp}(\Delta\mathbf{k})$ carries the specific pump mode that excites the nonlinear crystal. Using cylindrical coordinates (ρ,ϕ,z), where $dr^3 = \rho d\phi d\rho dz$, the integrals in (ρ,ϕ) in $\tilde{\psi}_{lp}(\Delta\mathbf{k})$ are performed giving [3]

$$\tilde{\psi}_{lp}(\Delta\mathbf{k}) = \pi A_{lp}(i/2)^l (z_R/k_P)^{1+l/2} e^{-il(\pi/2)} \rho_k^l L_l^p[(z_R/k_P)\rho_k^2] \times e^{-z_R/2k_P\rho_k^2} e^{il\arctan(\Delta k_y/\Delta k_x)} \int_{z_0-l_c/2}^{z_0+l_c/2} \times e^{-i\Delta k_z z} e^{(-1+l+2p)\arctan(z_R/z)} e^{i(1+l+2p)\arctan[z/(2z_R)]} dz, \quad (6)$$

where l_c is the crystal thickness. With the usual condition $z_R \gg l_c$, one obtains

$$\tilde{\psi}_{lp}(\Delta\mathbf{k}) = \pi A_{lp}(-1) i (i/2)^l (l_c z_R/k_P) e^{i(p\pi - z_0\Delta k_z)} \times e^{il\arctan(\Delta k_y/\Delta k_x)} e^{-\xi/2} \xi^{l/2} L_l^p(\xi) \frac{\sin(l_c\Delta k_z/2)}{(l_c\Delta k_z/2)}, \quad (7)$$

where $\xi = (z_R/k_P)\rho_k^2$ and $\rho_k = \sqrt{\Delta k_x^2 + \Delta k_y^2}$.

It should be observed that in the wave-vector space, one could identify $\arctan(\Delta k_y/\Delta k_x)$ with an angle φ_k associated with the signal and idler *pair*. Differently from the starting angle $\phi = \arctan(y/x)$ associated with the pump mode and $\mathbf{r}$-space variables, φ_k connects $\mathbf{k}$-space variables from signal and idler. In some simple cases (e.g., type I, degenerate case) $\varphi_k = (\varphi + \varphi')/2$, where φ and φ' are individual azimuthal angles for signal and idler in the wave-vector space, respectively, around the pump propagation direction—taken as the quantization axis.

This is a convenient point to discuss nonorthogonality of the signal and idler fields. Laguerre modes are orthogonal satisfying the relation $\int_0^\infty L_m^a(x) L_n^a(x) x^a e^{-x} dx = 0$ for $m \neq n$; one could ask, e.g., if $L_l^p(\xi)$ in Eq. (7) can be decomposed into products of Laguerre modes describing signal and idler as independent contributions. The negative answer can be physically understood due to the signal and idler entanglement. From the definitions of Δk_j and ξ, it can be seen that expansion of $L_l^p(\xi)$ into products of *independent* terms in $\mathbf{k}$ and $\mathbf{k}'$ cannot be done. Further processing or mode projections (filtering) of the SPDC generated light have to be applied to extract signal or idler in pure Laguerre modes [4].

$|\tilde{\psi}_{lp}(\Delta\mathbf{k})|^2$ is directly proportional to the crystal probability to generate signal and idler pairs with wave vectors $\mathbf{k}$ and $\mathbf{k}'$ given the paraxial incident pump field mode at $\mathbf{k}_P$ [as given by Eq. (5)]. In this theory, differently from usual treatments, the outgoing signal and idler fields are *not* limited to paraxial cases. It is understood that at each successful down-conversion event, the excited crystal decays onto a single-photon pair, along any emission directions $\mathbf{k}$ and $\mathbf{k}'$ allowed by conservation laws. These laws define the so-called phase matching conditions that specify maxima for Eq. (7). Basically, the maximum of $\sin(l_c\Delta k_z/2)/(l_c\Delta k_z/2)$ is given by values of the *longitudinal* variables $\Delta k_z = (\mathbf{k}+\mathbf{k}'-\mathbf{k}_P)_z$, while maximum of $e^{-\xi/2}\xi^{l/2}L_l^p(\xi)$ is given by values of the *transverse* variables connected to $\xi = (z_R/k_P)(\Delta k_x^2 + \Delta k_y^2)$. Both Δk_z and ξ will depend on the azimuthal angles *if* the refractive indexes have azimuthal dependence [3]. Whenever this dependence exists, the transfer of OAM from the pump beam to the down-converted photons may be frustrated as shown in [3,5]. The situation described in this work is *not* related to frustrated OAM transfer.

A normalized wave state describing *any* entangled photon pair from SPDC can be written [3]

$$\tilde{\psi}_{lp}(\xi)\rangle_n = \int_{\mathbf{k}} d^3k \int_{\mathbf{k}'} d^3k' \frac{A_{\text{amp}}^{(l,p)}}{\sqrt{\int_{\mathbf{k}} d^3k \int_{\mathbf{k}'} d^3k' |A_{\text{amp}}^{(l,p)}|^2}} |1_{\mathbf{k}}\rangle |1_{\mathbf{k}'}\rangle, \quad (8)$$

$A_{\text{amp}}^{(l,p)} = i(-1)^l e^{-\xi/2}\xi^{l/2} L_l^p(\xi) e^{il\arctan\Delta k_y(\mathbf{k},\mathbf{k}')/\Delta k_x(\mathbf{k},\mathbf{k}')} \frac{\sin(l_c\Delta k_z/2)}{(l_c\Delta k_z/2)}$, $\mathbf{k}'$ will be specified by phase matching according to $\mathbf{k}' = \mathbf{k_P} + \Delta\mathbf{k} - \mathbf{k}$ where $\Delta\mathbf{k}$ is taken at the value that maximizes $A_{\text{amp}}^{(l,p)}$. OAM indexes for signal and idler photons are *not* present in $|1_{\mathbf{k}}\rangle$ (say, l_s) or $|1_{\mathbf{k}'}\rangle$ (say, l_i). An OAM mode with index l has a *mode* signature distinct from a single plane-wave signature. In Eq. (8) the effect of the nonlinear polarizability $A_{\mathbf{k},\sigma;\mathbf{k}',\sigma'}$ has been neglected; it provides only smooth contributions along the down-converted rings.

In optical systems used to transmit or collect SPDC states, cases range from free-propagation geometry, where in a distance of, say $D = 10$ km, the wave-front dimension for a coincidence donutlike structure will spread by $\sim D \tan 0.01 \sim 100$ m and telescopic guidance is necessary

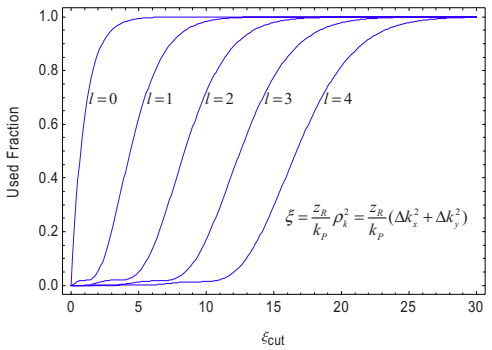

FIG. 2. (Color online) Used fraction of the scattered light as a function of ξ_{cut} for $l=0,1,2,3,4$.

(e.g., [6] with a simple $l=0$ case), Dove prisms [7] to select OAM modes ($l\neq 0$), and cases of small optical structures where microguidance is necessary [8] ($l\neq 0$).

In spherical coordinates $\mathbf{k}=\mathbf{k}(k,\varphi,\theta)$; imposing geometrical restrictions Δk, $\Delta\varphi$, and $\Delta\theta$ on the detected light field may lead to a poor mode distinguishability. Rough estimates can be done without specifying particular cases and involves direct considerations over ξ and Δk_z. However, it is hard to use this approach to map it onto specific cases. The variables ξ and Δk_z are related to structures in the signal and idler wave-vector space [3]. ξ connects variables (k,k',φ,φ') and constrains them by phase match in the nonlinear medium (see Ref. [3]). A detecting system that restricts too much the collection area (e.g., see area A_{cc} in Fig. 1) is not able to reveal the orbital angular-momentum value l associated to the incoming mode. An estimate of restrictions on the range of wave vectors collected is sketched in Fig. 2 for l values ranging from $l=0$ to $l=4$. This plot represents the magnitude *square* of the amplitude in Eq. (8) integrated from 0 to an arbitrary value of $\xi=\xi_{cut}$. This gives a good idea of the effect of a wave-vector cutoff. However, it should be emphasized that the calculation for specific geometries needs specific wave-vector boundaries and cannot be done with the compact ξ coordinate. A complementary view is shown in Fig. 3 where the abscissa axis gives the l values for the same range of ξ_{cut} values.

While Fig. 1 shows a general collecting area, particular shapes are involved in an experiment. Restriction in the collecting geometries may be exemplified by stops with azimuthal symmetry (see Fig. 4) or sector shapes that break this symmetry (see Fig. 5).

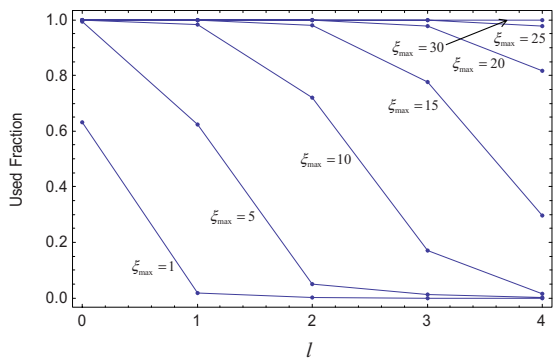

FIG. 3. (Color online) Used fraction of the scattered light as a function of l for some values of ξ_{cut} up to $\xi_{cut}=30$.

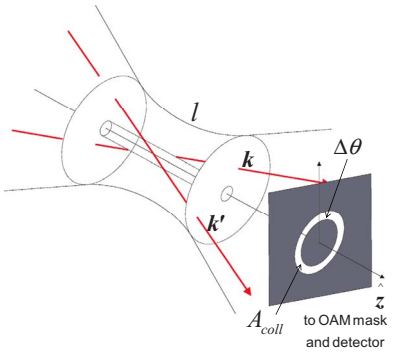

FIG. 4. (Color online) Stop with azimuthal symmetry.

Even using a correct OAM filter (e.g., a proper OAM mask) but with a **k**-restricting collection optics, some degree of indistinguishability appears. For simplicity, assume that one of the detecting systems (either signal or idler) detects the correct mode while the other has a restrictive collection optics as depicted in Figs. 4 and 5. Consider that a perfectly absorbing stop is being used in front of a detection system blocking a range of wave vectors from the generated SPDC. In a simplified way, the accepted fraction can be written

$$|\varphi_{lp}(\xi)\rangle_n=\int\!\!\!\!\!\!\frown_{\mathbf{k}} d^3k \int\!\!\!\!\!\!\frown_{\mathbf{k}'} d^3k' \frac{A_{\text{amp}}^{(l,p)}}{\sqrt{\int_{\mathbf{k}} d^3k \int_{\mathbf{k}'} d^3k' |A_{\text{amp}}^{(l,p)}|^2}} |1_{\mathbf{k}}\rangle \times |1_{\mathbf{k}'}\rangle, \tag{9}$$

where the symbol $\int\!\!\!\!\!\!\frown$ indicates a partial integration representing wave vectors allowed by the stopper (this simplification just tries to avoid OAM decomposition to describe the wave vectors reaching the detector). A measure of the overlap between these states is

$$F(\rho_{\tilde{\psi}},\rho_{\varphi})\equiv|\langle\rho_{\tilde{\psi}}|\rho_{\varphi}\rangle|=\frac{\int\!\!\!\!\!\!\frown_{\mathbf{k}} d^3k \int\!\!\!\!\!\!\frown_{\mathbf{k}'} d^3k' |A_{\text{amp}}^{(l,p)}|^2}{\int_{\mathbf{k}} d^3k \int_{\mathbf{k}'} d^3k' |A_{\text{amp}}^{(l,p)}|^2}. \tag{10}$$

The fraction represented by Eq. (10) represents the best possible identification of the generated wave state due to partial

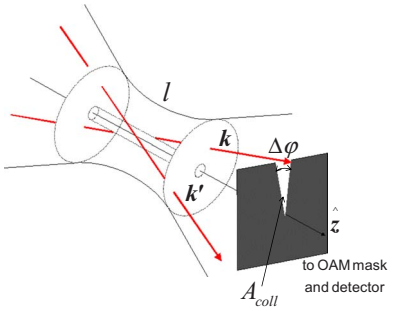

FIG. 5. (Color online) A stop without azimuthal symmetry.

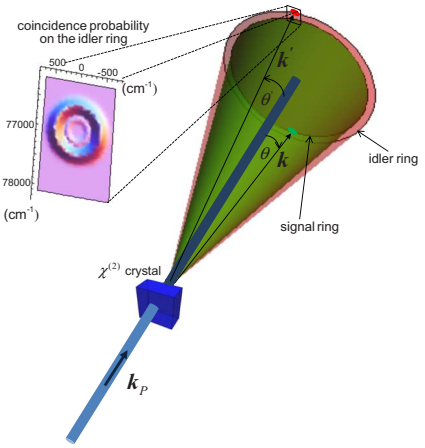

FIG. 6. (Color online) A $\chi^{(2)}$ crystal is pumped by a uv laser mode at $\lambda_P=3511$ Å, with OAM $l=2$. Type I signal and idler rings and the calculated coincidence structure at the idler position (wave-vector space) given that a signal photon has been detected at **k**. The coincidence structure corresponds to OAM $l=2$. The ring angles are at $\theta_0=0.49$ rad and $\theta_0'=0.54$ rad.

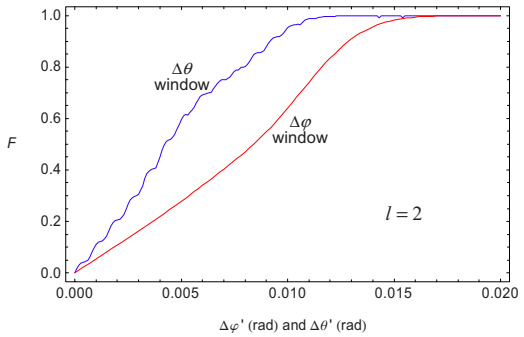

FIG. 7. (Color online) Overlap due to idler wave-vector restrictions. In these examples, annular or sector openings allow light collection and block outside the openings.

detection imposed by the detecting geometries. As a simple example, assume that a nonlinear crystal has been excited by a laser mode carrying OAM l and a down-converted *signal* photon has been detected at a particular wave vector **k**. It is also assumed that this interaction has azimuthal symmetry by considering type I SPDC [5]. The assumption of a specific **k** vector (a plane wave) implies that this photon has $l_s=0$ and, therefore, the *idler* photon has to carry the OAM $l_i=l$ [5]. However, the detecting system for the idler photon has to allow detection of a range of wave vectors that, *in principle*, could reveal that the single idler photon could belong to an OAM mode. Restrictions on the wave vectors collected will be imposed by the use of stoppers either with azimuthal symmetry (see Fig. 4) or without azimuthal symmetry (see Fig. 5). As an example, a type I crystal potassium titanium oxide phosphate (KTP) is chosen with ordinary refractive indexes for signal and idler photons, pump-laser wavelength $\lambda_P=3511$ Å with OAM $l=2$, signal $\lambda_s=6328$ Å and idler $\lambda_i=6870$ Å; and $l_c=0.2$ cm and $z_R=10$ cm. Angles internal to the medium will be considered for simplicity (Snell's law easily give external angles). Polar angles θ and θ' for signal and idler that maximize the amplitude $A_{\text{amp}}^{(l,p)}$ can be found numerically. They give the position of the signal and idler rings at their maximum amplitudes. Choosing $\varphi=0$ around the signal ring as the wave-vector position where a signal photon is found and looking around the $\varphi'=\pi$ on the idler ring, the coincidence structure given by $|A_{\text{amp}}^{(l,p)}|$ is calculated. Figure 6 shows the signal and idler rings and the calculated coincidence structure at the idler position. Figure 7 shows F for a stopper allowing light within annular rings centered around the idler ring as a function of spreads $\Delta\theta$ and for a stopper allowing light in sectors with openings $\Delta\varphi$. Figure 7 summarizes the obtained results, where the overlap F represents the maximum allowable information that can be obtained due to geometrical restrictions. Differently from identifying polarization states, OAM states demand that a set of wave vectors could be detected to allow reasonable identification of the precise OAM value attached to the mode. This is the case when repeated mode preparations are possible or even when a single sampling is allowed [9]. In Ref. [9], no detail on geometrical restrictions can be extracted and were—in fact—of no interest, differently from the results of the present Brief Report. A study of modifications introduced by the use of spatial light modulators on the detection path of SPDC can be seen in [10] aimed to the study of Fourier relationship between angle and angular momentum. These results call the attention to the fact that when designing a collecting system for OAM modes, a careful consideration of the range of wave vectors has to be taken into account. Application for any other l value is straightforward.

This work was supported by the U. S. ARO MURI under Grant No. W911NF-05-1-0197 on Quantum Imaging.

[1] L. Mandel and E. Wolf, *Optical Coherence and Quantum Optics* (Cambridge University Press, New York, 1995).
[2] L. Allen, M. W. Beijersbergen, R. J. C. Spreeuw, and J. P. Woerdman, Phys. Rev. A **45**, 8185 (1992).
[3] G. A. Barbosa, Phys. Rev. A **76**, 033821 (2007).
[4] A. Mair, A. Vaziri, G. Weihs, and A. Zeilinger, Nature (London) **412**, 313 (2001).
[5] H. H. Arnaut and G. A. Barbosa, Phys. Rev. Lett. **85**, 286 (2000).
[6] R. Ursin, F. Tiefenbacher, T. Schmitt-Manderbach, H. Weier, T. Scheidl, M. Lindenthal, B. Blauensteiner, T. Jennewein, J. Perdigues, P. Trojek, B. Ömer, M. Fürst, M. Meyenburg, J. Rarity, Z. Sodnik, C. Barbieri, H. Weinfurter, and A. Zeilinger, Nat. Phys. **3**, 481 (2007).
[7] J. Leach, J. Courtial, K. Skeldon, S. M. Barnett, S. Franke-Arnold, and M. J. Padgett, Phys. Rev. Lett. **92**, 013601 (2004).
[8] G. A. Barbosa, Phys. Rev. A **73**, 052321 (2006).
[9] G. A. Barbosa, Opt. Lett. **33**, 2119 (2008).
[10] A. K. Jha, B. Jack, E. Yao, J. Leach, R. W. Boyd, G. S. Buller, S. M. Barnett, S. Franke-Arnold, and M. J. Padgett, Phys. Rev. A **78**, 043810 (2008).